Self-organized critical random Boolean networks

Bartolo Luque, Fernando J. Ballesteros, and Enrique M. Muro
Centro de Astrobiología (CAB) INTA-CSIC, Carretera de Ajalvir km. 4, 28850 Torrejón de Ardoz, Madrid, Spain
(Received 25 October 2000; revised manuscript received 25 January 2001; published 25 April 2001)

Standard random Boolean networks display an order-disorder phase transition. We add to the standard random Boolean networks a disconnection rule that couples the control and order parameters. In this way, the system is driven to the critical line transition. Under the influence of perturbations the system points out self-organized critical behavior. Several numerical simulations have been done and compared with a proposed analytical treatment.

DOI: 10.1103/PhysRevE.63.051913 PACS number(s): 87.23.Ge, 87.23.Kg, 05.65.+b

I. INTRODUCTION

Random Boolean networks (RBN) were proposed [1] as discrete genetic network models. The network is composed of nodes (automata). The state of an automaton represents the state of a gene with two possible values (on-off). This state is the output of a Boolean function, which has the output activity of some other genes as inputs. The connectivity of the system and the bias used for the Boolean functions are relevant parameters in order to statistically determine the network dynamics. If the system has a high connectivity and a low bias, the dynamics of the automata is disordered; it seems that there is no correlation between the gene switching on and off. On the other hand, the dynamics is ordered if a low connectivity and a high bias are used. Only the ordered dynamics have biological sense. Kauffman says that this parametric region offers *free order* and it seems that natural selection works where the order existed previously [2]. In the critical region, which is the boundary between ordered and disordered phase, there are some scaling relations that have been the subject of recent works [3–5]. Kauffman points out that genetic networks evolve to the boundary between order and disorder. In this region there is more diversity of patterns for activity and greater possibilities for complex evolution (antichaos hypothesis) [6].

There is great interest in the evolution of topology in networks [7,8]. Several schemes have been proposed for RBN evolution. For instance, in [9] a RBN evolves from an initial $K=1$ mean connectivity (using a random initial condition) to an attractor. At this point a copy of the network is made that has a connection randomly removed or/and added. The new network also reaches an attractor. If the same attractor has been obtained, the network is maintained. Otherwise, the previous one is restored. During the RBN evolution, it appears some stasi periods and punctuations like in real evolutionary processes.

In [10] the performance of an automaton is defined as the number of steps that it is in majority during a given set of steps. An automaton in majority means that it has the same state as the majority of the automata. The automaton with the highest performance is replaced by another automaton with a new random Boolean function and the process is repeated. The authors show how the genetic network is able to modify its bias in order to reach the critical region.

In [11] is presented a method that is able to lead the connectivity of binary neural networks to their critical value. These neural networks have a phase transition similar to RBN [12,13]. Using a fixed connectivity initialization the network evolves to an attractor. If an automaton does not change its state in the attractor, a connection is added to it. Otherwise, if it changes then a connection is removed. The different networks (with different initial connectivities) reach and remain close to the critical region.

From a more general perspective, some works [14–18] have shown the relation between critical and self-organized critical phenomena. In particular, Sornette *et al.* [18] point out a heuristic method that transforms a system with a critical transition (Ising or bond percolation) into a self-organized critical system. They propose to add some kind of mechanism (a feedback between the order and control parameters) that slowly drives the system towards the critical point.

RBN are a classical example where complex global behavior emerges from local simple rules. They exhibit a phase transition similar to the Ising model or bond percolation. Forgetting its initial biological inspiration, our goal is to develop RBN that spontaneously evolve towards a global critical stationary state. For this purpose we use a disconnection rule that induces a feedback between the control and order parameters. These networks reach a critical state without changing externally the control parameter. These systems show characteristics related to self-organized criticality. Our evolution method is distinct from earlier works in the following: we introduce a well-defined coupling between order and control parameters as in [11], but the method is able to stabilize (the individuals connectivities become constant in time) the networks along the critical curve.

In Sec. II we give an introduction to RBN and we present the disconnection local rule that gives to the RBN a self-organized critical (SOC) behavior. In Sec. III statistical results of the evolution of the self-organized RBN are presented. In Sec. IV we show its SOC behavior in response to external perturbations. In Sec. V we apply an analytical treatment to the model and discuss the results, and finally, in Sec. VI we make a summary and point out issues for future works.

II. HOW DOES ONE MAKE A CRITICAL SELF-ORGANIZED RBN?

A RBN is a discrete dynamical system composed of N automata. Each automaton is a Boolean variable with two

possible states: $\{0,1\}$, such that

$$\mathbf{F}:\{0,1\}^N \mapsto \{0,1\}^N, \tag{1}$$

where $\mathbf{F}=(f_1,\ldots,f_i,\ldots,f_N)$ and each f_i is a Boolean function of K_i inputs (the automaton i is connected to K_i automata randomly chosen from the set of N automata)

$$f_i:\{0,1\}^{K_i} \mapsto \{0,1\}. \tag{2}$$

An automaton state $x_i^t \in \{0,1\}$ is updated using its corresponding Boolean function

$$x_i^{t+1}=f_i(x_{i_1}^t, x_{i_2}^t, \ldots, x_{i_{K_i}}^t). \tag{3}$$

Each f_i is represented as a look-table of K_i inputs. Initially, K_i neighbors and a look-table of bias p are assigned to each automaton. In order to generate such a look-table, the value 1 is assigned to an output with a probability p and 0 with a probability $1-p$. When the neighborhood and the functions are established, they are maintained (quenched).

We randomly initialize the states of the automata (initial condition of the RBN). The automata are updated synchronously using its corresponding Boolean functions

$$\mathbf{x}^{t+1}=\mathbf{F}(\mathbf{x}^t), \tag{4}$$

These RBN exhibit a second-order phase transition [19]. The control parameters (K and p) determine two regions: a frozen phase for $K<1/2p(1-p)$ and a disordered phase for $K>1/2p(1-p)$. Thus, the critical boundary is represented as follows:

$$K_c(p)=\frac{1}{2p(1-p)}. \tag{5}$$

The above description corresponds to a classical RBN. We incorporate a disconnection rule to the system leading the RBN to a stationary critical state with connectivity $K_c(p)$ [see Eq. (5)]. The rule is also applied synchronously to each automaton i that has a local connectivity $K_i(t)$ in such a way that: (1) disconnection threshold; if $K_i(t)>2$ then

$$K_i(t+1)=\begin{cases} K_i(t)-1 & \text{if } \sum_{j=1}^{K_i(t)} x_{i_j} < K_i(t)-1 \\ K_i(t), & \text{otherwise;} \end{cases} \tag{6}$$

(2) minimal connectivity; if $K_i(t)=2$ then

$$K_i(t+1)=K_i(t). \tag{7}$$

The rule is inspired in the Bak-Tang-Wiesenfeld model [20]. As in the sandpilelike model we have incorporated a threshold. If the number of 0's in the input of a Boolean function is greater than one and the local connectivity of its corresponding automaton is $K_i(t)>2$, a connection of this automaton (randomly chosen) will be cut. Then, a new Boolean function with connectivity $K_i(t)-1$ will be assigned.

The disconnection mechanism is illustrated in Fig. 1. The automaton i has a connectivity $K_i(t)=3$ and an input vector composed by two $0's$ and one 1. Hence, a random connection is cut $[K_i(t+1)=2]$ and another Boolean function with bias $p=0.5$ is assigned. A new state is then computed.

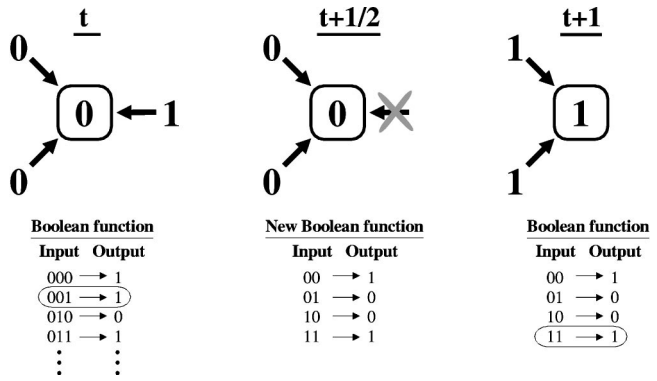

FIG. 1. Disconnection of an automaton i with $K_i(t)=3$. The automaton receives more than one 0. At $t+1/2$ one of the automaton connections is randomly cut and its Boolean function is changed (by a look-table with bias $p=0.5$). The new Boolean function obtains a new state for the automaton in $t+1$.

In a sandpilelike system there is a decrease in the mass, energy, tension, etc. at the boundaries [20,21]. In the proposed RBN, there is a decrease in the number of connections. Our system is a random graph with no boundaries. But, there is a diffusion effect that is able to cause an avalanche of disconnections. If one automaton connection is cut (at t), its state can change from 1 to 0 (at $t+1$). The last change may cause a disconnection (at $t+1$) in any of the automata that are connected to the first one, and so on until a stationary state is reached.

III. RESULTS

The average of the evolution of the mean connectivity $K(t)$ of 1000 RBN, each one with $N=10\,000$ automata, is represented in Fig. 2. Each RBN diminishes its connectivity due to Eqs. (6) and (7). A fixed bias p has been used for every RBN: 100 different RBN and for each one 10 initial conditions of the automata states (50% of $1's$ and 50% of $0's$ approximately). All the RBN automata have a connectivity $K_i(t=0)=10$. The bias p ranges from 0.5 to 0.9 in steps of 0.01. The stationary state (when no more connections are cut) is quickly reached in about 50 iterations. The mean connectivity $K(t)$ stabilizes close to the transition curve between order and disorder $[K_c(t)]$. This curve is determined by Eq. (5) and it is represented as a continuous line in Fig. 3. In the same figure, the circles are the stationary result of the averaged mean connectivity (corresponding to section p versus K at $t=100$, in Fig. 2). It can be observed that the RBN stabilizes at the transition curve. In the same figure, three instances of the evolution of three RBN ($p=0.50$, $p=0.70$ and $p=0.85$) have been represented. The fill-down triangles represent the values of the RBN mean connectivity evolving towards equilibrium. In addition the pattern evolution of the above three examples are represented in Fig. 4.

The self-overlap $a(t)$ is the unitary percentage of automata with the same value in $t-1$ and in t. The stationary

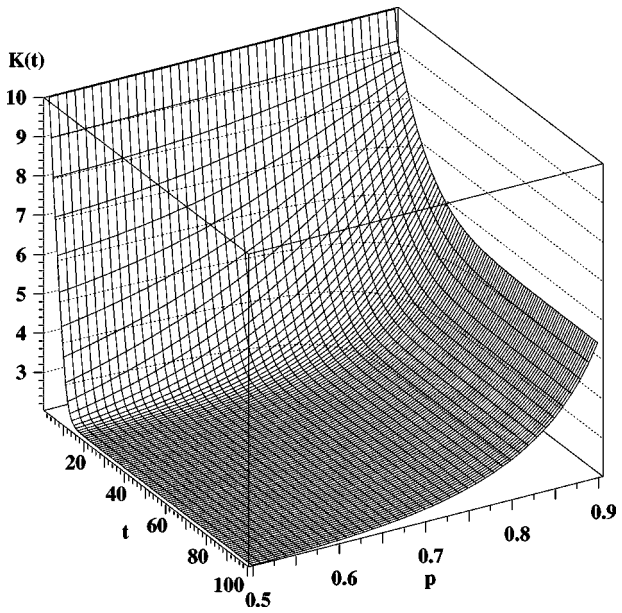

FIG. 2. Average evolution of the mean connectivity $K(t)$, where t are the iterations. We have considered 1000 RBN ($N=10\,000$): 100 different RBN with 10 initial conditions (50% of the automata with state 1 and 50% with state 0 in $t=0$) for each value of the bias p. All the RBN have a initial $K(t=0)=10$ mean connectivity.

self-overlap, $a(t\rightarrow\infty)=a^*$, is an order parameter for the RBN transition [22]. Therefore in the disordered state we have $a^*<1$ and in the ordered state the self-overlap is given by $a^*=1$. In Fig. 5 we have represented the self-overlap evolution (averages are calculated as in Fig. 2). The initial

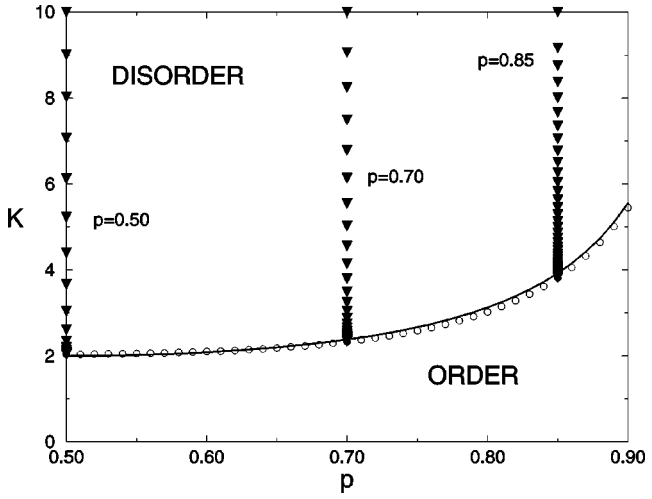

FIG. 3. (a) The continuous line represents the critical curve obtained from the theory [Eq. (5)]. It is a boundary between the ordered and disordered phases of the RBN. (b) The fill-down triangles represent three instances of the RBN evolution for $p=0.50$, $p=0.70$, and $p=0.85$. Each triangle represents the mean connectivity $K(t)$ in consecutive steps. (c) The circles represent the stationary state at the end of the RBN evolution $[K(t=0)=10]$ using different values for the bias p (ranging from $p=0.5$ to $p=0.9$ in p increments of 0.01). Each circle represents the average of 1000 RBN ($N=10\,000$) during 1000 time steps.

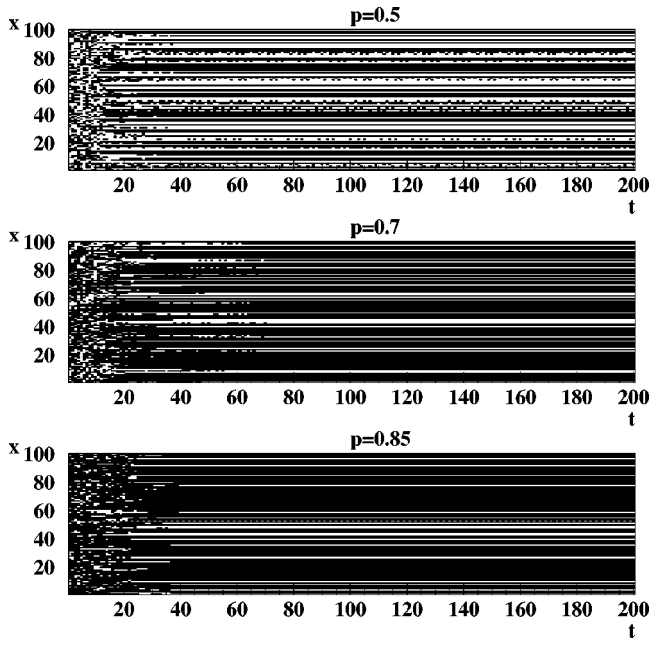

FIG. 4. These figures show the spatiotemporal automata activity for the evolution of networks built of $N=100$ automata. Time runs from left to right. The number of iterations is represented by t. The value of the automaton state (vertical axis) is represented as black if it is one, and white otherwise. From top to bottom: RBN with $p=0.50$, $p=0.70$, and $p=0.85$.

self-overlap is $a(t=1)=0.5$ due to the random state initialization. It can be observed that the self-overlap grows quickly reaching the stationary value $a^*=1$ for high values of the bias. This is to be expected because in the critical boundary with $K=K_c$, the self-overlap reaches the value $a(t)=1$ for the first time. On the other hand, for low values of the bias, the self-overlap is stable at a value lower than 1. We will show in Sec. V that this is an RBN size effect.

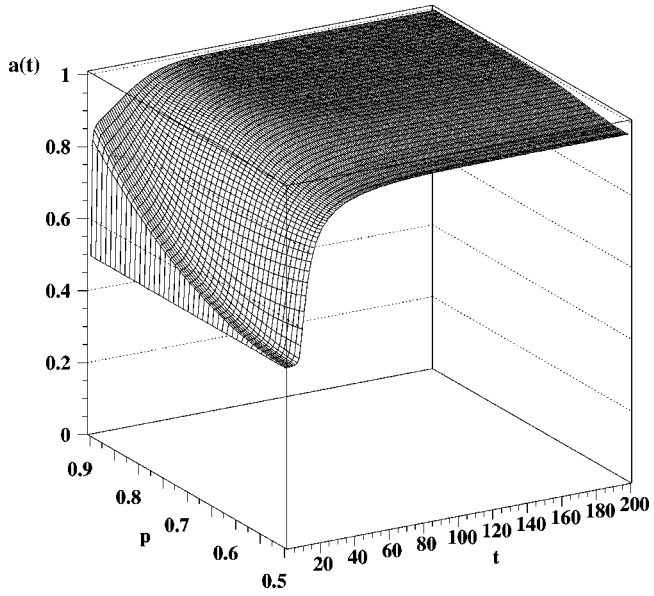

FIG. 5. Evolution of the average self-overlap $a(t)$ for the simulations of Fig. 2 (t is the number of iterations).

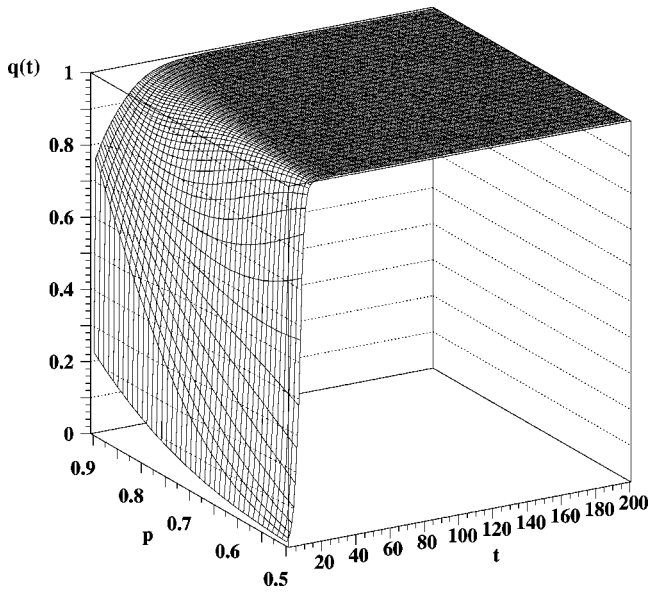

FIG. 6. Average self-overlap of the connectivity $q(t)$ for the simulations in Fig. 2 (t is the number of iterations).

In order to compare the different velocities to approach the stability in the self-overlap and the connectivity, the self-overlap of the connectivities $q(t)$ has been represented in Fig. 6. The quantity $q(t)$ is defined as the unitary percentage of automata that have the same connectivity at times $t-1$ and t. As it can be observed, the connectivity is stabilized, approximately, in 50 time steps. On the other hand, the self-overlap needs about 100 time steps to stabilize.

In short, the evolution of an RBN with dynamics given by Eqs. (6) and (7) is such that the RBN is driven from the disordered phase to the critical boundary [Eq. (5)] with mean connectivity $K_c(p)$ and self-overlap $a \approx 1$.

In the next section we study the nature of the RBN equilibrium state, and whether it is metastable or not. In order to do so we analyze the response of the system to external perturbations.

IV. PERTURBATION ANALYSIS

We now evolve the RBN using the disconnection rule [Eqs. (6) and (7)]. We perturb the RBN making use of sandpilelike methods [20,21]. For this purpose we start with a relaxed RBN and a fixed bias p. In order to perturb the RBN, we randomly choose an automaton i, and add to it a connection (i.e., its connectivity changes from K_i to K_i+1). A new Boolean function f_i with K_i+1 inputs is assigned to i using the bias p, so that one obtains a new state for the automaton i. If the automaton state is maintained, then there is only a small increase in the RBN mean connectivity. If the automaton state changes, it is possible to cause a disconnection, originating an avalanche via branching. When the avalanche stops, the RBN is minimally perturbed again, and so on.

In order to characterize the avalanches, we have measured two different variables: the time T needed for the net to reach a stationary state and the total number of disconnections B during T. In Fig. 7 the histogram $S(T)$ of avalanche times is

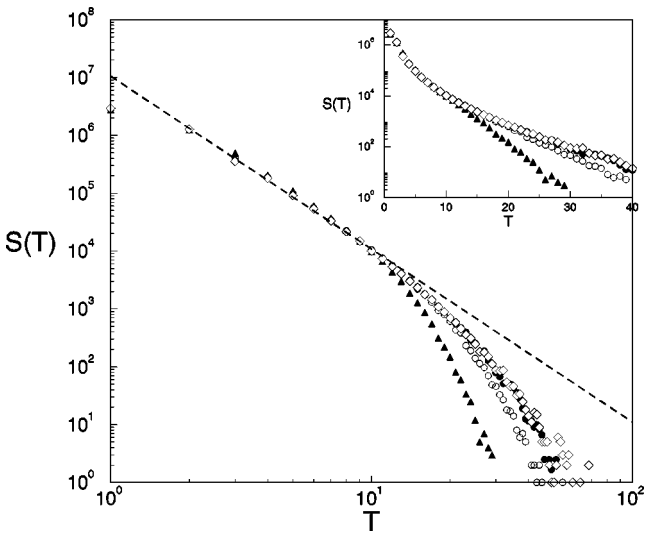

FIG. 7. Log-log histogram $[S(T)]$ for T (iterations needed for the system to reach a stationary state) during 5×10^6 perturbations in a RBN. $p=0.65$ for $N=100\,000$ (diamonds), $N=10\,000$ (filled circles), $N=1000$ (unfilled circles), and $N=100$ (triangles). Inset: the same figure but in linear-log form.

represented after 5×10^6 perturbations. For this purpose we have used a RBN with $p=0.65$ and different sizes: $N=100$ (triangles), $N=1000$ (unfilled circles), $N=10\,000$ (filled circles), and $N=100\,000$ (diamonds). The dotted line is a visual guide to see the size effect. It is easy to see that when $N\to\infty$, the histograms tend to a power law. A fit with the first points gives $S(T)\sim T^z$ with $z=-2.9\pm0.1$. Figure 8 shows the histogram $S(B)$ of disconnections using the same numerical simulations as before. We obtain again a possible power law described by $S(B)\sim B^D$ with $D=-2.2\pm0.2$. In both figures, insets in linear-log form are showed in order to exclude possible exponential fits.

In the inset of Fig. 9 we show the temporal evolution of

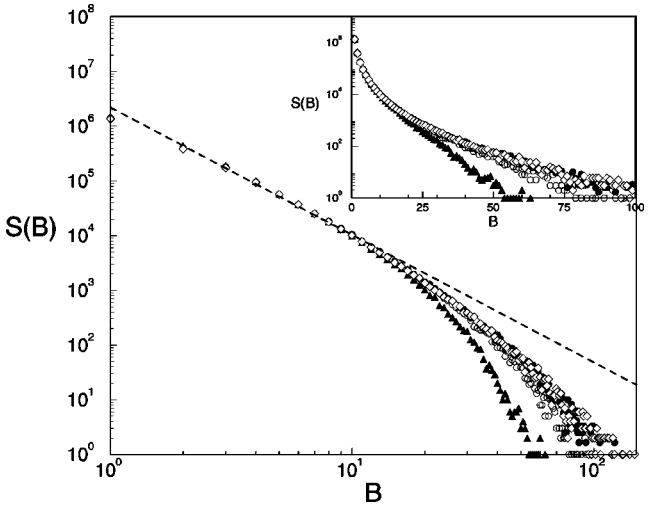

FIG. 8. Log-log histogram for the sizes of the avalanches B. B is the number of disconnections for each perturbation and $S(B)$ is the histogram. For this purpose, it has used the same simulations of Fig. 7. Inset: the same figure but in linear-log form.

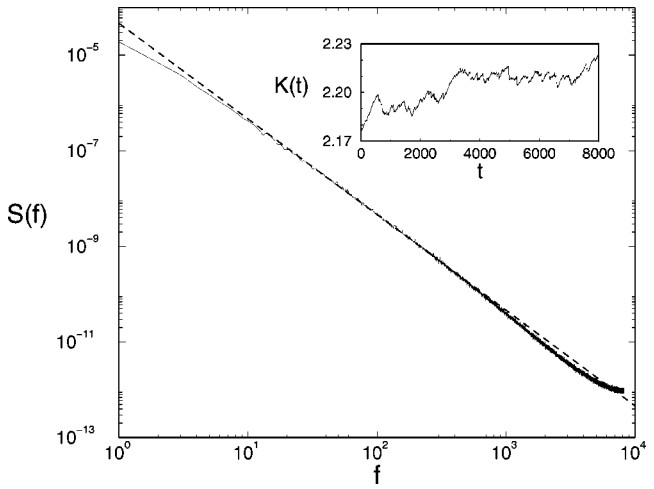

FIG. 9. Power spectrum (log-log) of the mean connectivity evolution $K(t)$ of a RBN ($p=0.65$ and $N=10\,000$). It is the average of 305 temporal series of 16 384 steps. The slope of the dotted line is $\phi=-1.92\pm0.09$. Inset: a particular case of the evolution of the mean connectivity $K(t)$ for the average series (t is the number of iterations).

the mean connectivity $K(t)$ for a perturbed RBN ($N=10\,000$, $p=0.65$). In Fig. 9 we represent the power spectrum $S(f)$ (log-log) obtained by averaging 305 temporal series of 16 384 time steps. A power law described by $S(f)\sim f^{\phi}$ with $\phi=-1.92\pm0.09$ is in good agreement with the data.

The numerical results do not seem definitive. The power-law regime for T and B lasts for almost a decade, but there is a clear finite size effect. There are strong computational restrictions for working with bigger RBN because the size of the avalanches is limited by the number of RBN automata. Nevertheless, in the $S(f)$ histogram there is scaling for more than two decades. In conclusion, we think that the results point out a SOC behavior.

V. ANALYTIC TREATMENT

At this point we ask ourselves: why are the evolution rules able to drive an RBN to the critical boundary between the order and disorder phases? As the bias has been already fixed, there can only be variations in the mean connectivity $K(t)$ (acting as order parameter) and the self-overlap $a(t)$ (control parameter). In this section we show that there is a feedback mechanism between both parameters that leads the system to a SOC behavior [18].

As we mentioned before, the self-overlap $a(t)$ is the unitary percent of automata that has the same state in $t+1$ and t. If the mean connectivity $K(t)$ is known, the value of the self-overlap at time $t+1$ can be determined by the following equation:

$$a(t+1)=a^{K(t)}(t)+\mathcal{P}(1-a^{K(t)}(t)). \tag{8}$$

If we interpret $a(t)$ as the probability for an arbitrary automaton to remain in the same state at both $t-1$ and t, the term $a^{K(t)}(t)$ gives the probability that all the inputs of a given automaton are the same for $t-1$ to t. It is clear that $1-a^{K(t)}(t)$ is the probability that at least one of the inputs will be different at t and $t-1$. In that case, there is still a probability that this particular automaton remains in the same state at t and $t+1$ by chance. This probability is given by $\mathcal{P}=p^2+(1-p)^2$ [22]. In a standard RBN the mean connectivity K does not have an explicit dependence on time. If one includes the disconnection rule described above, the mean connectivity of the system evolves with time. If $P_k(t)$ is the probability of an automaton to have connectivity k, then

$$K(t)=\sum_{k=2}^{10}P_k(t)k, \tag{9}$$

where the maximum connectivity value has been taken as 10, without loss of generality. The connectivity distribution evolves according to the following system of equations:

$$P_{10}(t+1)=[\Phi_{10}+(1-\Phi_{10})a^{10}(t)]P_{10}(t), \tag{10a}$$

$$P_k(t+1)=(1-\Phi_{k+1})[1-a^{k+1}(t)]P_{k+1}(t)+[\Phi_k+(1-\Phi_k)a^k(t)]P_k(t), \tag{10b}$$

$$P_2(t+1)=(1-\Phi_3)[1-a^3(t)]P_3(t)+P_2(t), \tag{10c}$$

where $k=9,8,\ldots,3$. The variable $\Phi_k=p^k+kp^{k-1}(1-p)$ is the automaton probability to maintain its connectivity by chance. Equation (10a) describes the loss of connections for all the automata with connectivity 10 at instant t. The rest of the Eqs. (10b), except for the last one [Eq. (10c)], have two contributions: the first one represents the creation of automata with connectivity k that previously had connectivity $k+1$, and the second one describes the automata that maintain their same value of connectivity k. The last equation [Eq. (10c)] describes the growth of automata population with connectivity 2. The evolution of the critical self-organized RBN is described by the coupled system of Eqs. (8) and (10a)–(10c).

One can see that $a^*=1$ is the only possible value that makes the probability distribution stationary. In Eq. (8), $a^*=1$ is a fixed point when $K^*(1-\mathcal{P})\leqslant 1$, where $K^*=K(t\rightarrow\infty)$ is the asymptotic connectivity, that is, whenever the stationary mean connectivity satisfies

$$K^*\leqslant\frac{1}{2p(1-p)}, \tag{11}$$

whose boundary is the critical curve depicted in Fig. 3. From the system of Eqs. (10a)–(10c) it can be easily deduced that

$$K(t+1)=K(t)-[1-P_2(t)]-\sum_{k=3}^{10}[\Phi_k+(1-\Phi_k)a^k(t)]P_k(t), \tag{12}$$

so that the mean connectivity of the system always decreases during its dynamical evolution. Therefore, if the initial condition satisfies $K(t=0)>1/[2p(1-p)]$, it will slowly fall

towards the critical condition. The first time $a^*=1$ is when the system reaches the critical curve and it therefore stabilizes.

We can study more rigorously the evolution of the system by the classical analysis of linear stability. We perturb the fixed point $\Omega^* \equiv (a^*=1, P_{10}^*, \ldots, P_k^*, \ldots, P_2^*)$, with $K^* = \Sigma_{k=2}^{10} P_k^* k$, and compute the Jacobi matrix of the system at Ω^*:

$$\mathbf{L}(\Omega^*) = \begin{pmatrix} K^*(1-\mathcal{P}) & 0 & \cdots & 0 & \cdots & 0 \\ 10(1-\Phi_{10})P_{10}^* & 1 & \cdots & 0 & \cdots & \vdots \\ \vdots & \vdots & \ddots & \vdots & \vdots & \vdots \\ k(1-\Phi_k)P_k^* & & & & & \\ -(k+1)(1-\Phi_{k+1})P_{k+1}^* & \cdots & \vdots & 1 & \cdots & \vdots \\ \vdots & \cdots & \vdots & \vdots & 1 & 0 \\ -3(1-\Phi_3)P_3^* & 0 & 0 & 0 & 0 & 1 \end{pmatrix}. \tag{13}$$

We can calculate the characteristic polynomial by means of the determinantal condition

$$|\mathbf{L}(\Omega^*) - \lambda \mathbf{I}| = 0. \tag{14}$$

Thus,

$$P(\lambda) = [K^*(1-\mathcal{P}) - \lambda](1-\lambda)^9 = 0, \tag{15}$$

and then the associated eigenvalues are $\lambda_1 = K^*(1-\mathcal{P})$ and the (9 times) degenerated eigenvalue $\lambda_2 = 1$. This means that for $\lambda_1 \leqslant 1$ the critical point will indeed be linearly stable. One can see that the characteristic polynomial is independent of the stationary distribution $\{P_k^*\}$. Obviously this distribution depends on the initial conditions, but fulfills the condition $K^* = \Sigma_{k=2}^{10} P_k^* k$ and thus the condition (11).

In order to check this theoretical analysis we have performed several numerical simulations. In Fig. 10 the theoretical evolution of the self-overlap $a(t)$ has been represented with continuous line. We have used the following values: $a(t=0)=0.5$, $p=0.5$, and $P_k(t=0)=0.0$ for all k but $P_{10}=1.0$, that is, $K(t=0)=10$. It can be seen that the self-overlap converges asymptotically to 1. With the same parameters and initial conditions we have performed our set of numerical simulations. In the same figure we have also plotted the average evolution of the self-overlap for 1000 RBN of different sizes: $N=10\,000$ (circles), $N=1000$ (triangles), and $N=100$ (squares). As can be seen from the plot, the first steps of the simulation agree with the theoretical curve. It can be observed that the stationary state of the simulations approaches the theoretical one as N increases. In order to perform a scaling size effect study we have represented the stationary states $(1-a^*)$ for different sizes (see the inset in Fig. 10). The fitting shows that $(1-a^*) \sim (1/N)^{\alpha}$ with $\alpha = 0.27 \pm 0.05$, in such a way that in the thermodynamic limit $(N \to \infty)$ we get $a^*=1$, as is to be expected.

In a similar way, the four graphs in Fig. 11 show the theoretical evolution (continuous line) and the numerical simulation (circles) of the overlap for RBN ($N=10\,000$). For each graph we have used 1000 averaged simulations and four different values for the bias p. In Fig. 12 we have plotted the evolution of the theoretical $K(t)$ mean connectivity (lines) and simulations with RBN (symbols) for the same bias values of Fig. 11. Finally, in Fig. 13 we show $\{P_k^*\}$ the stationary distributions as functions of the bias p: theoretical (top one) and simulation (bottom).

From the previous figures it can be clearly observed that the computer RBN simulations agree with our theoretical analysis in spite of the size effect that is due to computational restrictions.

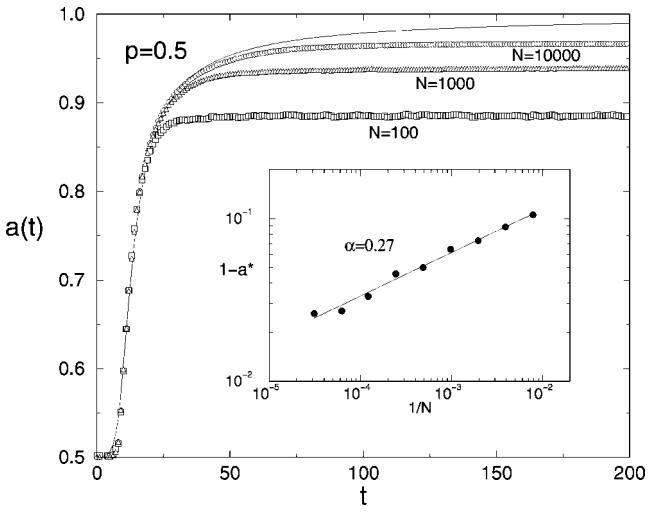

FIG. 10. The theoretical evolution of the self-overlap in a RBN. Where t is the number of iterations. $p=0.5$, $a(t=0)=0.5$, and $K(t=0)=10$. All the automata have connectivity 10, i.e., $P_{10}(t=0)=1.0$ (continuous line). The circles correspond to the numerical simulation for $N=10\,000$, the triangles for $N=1000$ and the squares for $N=100$. In the inset, the filled circles represent the average stationary values of the self-overlap reached by the RBN with different sizes, and logarithmically spaced out.

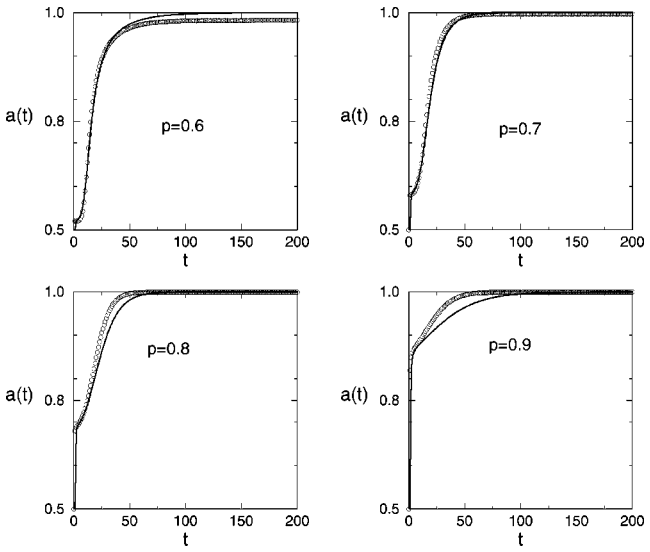

FIG. 11. Theoretical evolution (continuous line) and numerical simulation (circles) of $a(t)$ for RBN ($N=10\,000$). We have performed 1000 averaged simulations with four different values for the bias p (t is the number of iterations).

VI. SUMMARY

RBN are classic complex systems that show that global order is able to emerge from local rules. They exhibit a phase order-disorder transition modulated by the values of their connectivity and bias. Some authors have already proposed mechanisms for RBN evolution [9–11]. We have, following the Sornette *et al.* criterium [18], coupled the control parameter (connectivity for a fixed bias) and the order parameter (self-overlap) in order to convert a critical system into a self-organized critical one. From the numerical simulations it can be deduced that the system evolves from the disordered phase to the critical transition curve independently of the fixed bias. Moreover, the response to external perturbations points to a SOC behavior.

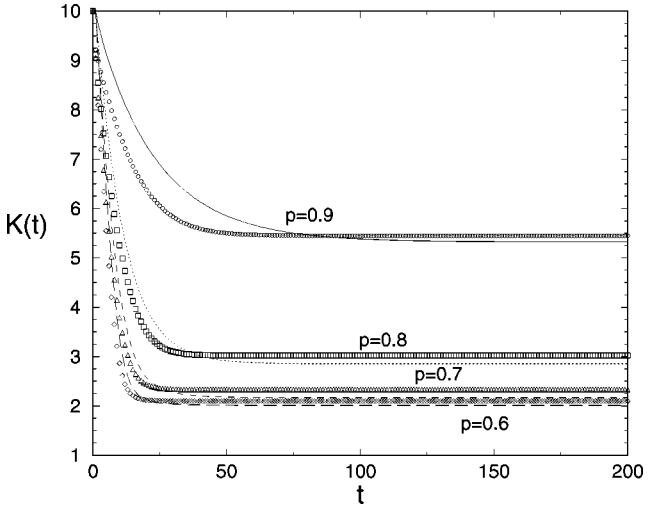

FIG. 12. Evolution of the mean connectivity $K(t)$ (t is the number of iterations): the lines correspond to the theoretical results and the symbols to the averaged simulations. We have considered the same cases as in Fig. 11.

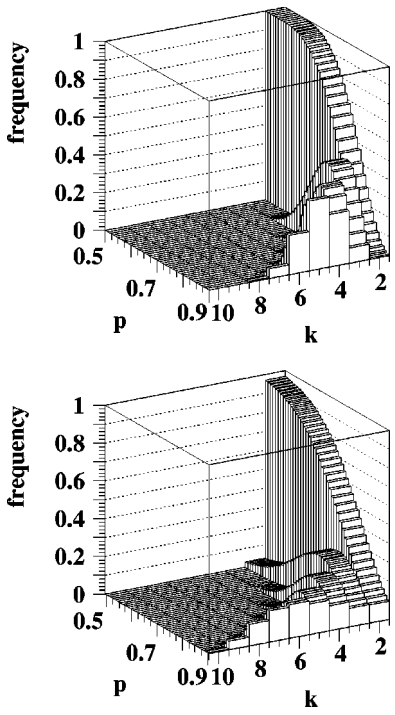

FIG. 13. Stationary distribution of the connectivity $P^*(k)$ with $k=2,3,\ldots,10$. In the bottom graph each distribution has been calculated averaging over 1000 RBN. In the top one we show the theoretical stationary distribution of connectivities.

The theoretical analysis fits with the numerical simulations and it is able to predict RBN behaviors to govern variations. We tested other disconnection rules (similar to 6 and 7): for example, we changed the breaking threshold of a connection. If there is a disconnection when no 0 inputs arrive to the automata, the system stabilizes under the critical curve. If there is a disconnection when there are more than one 0 inputs in the automata, the system stabilizes over the critical curve. In the theoretical analysis, these modifications imply that the probabilities Φ_k change. In the first case the probabilities increase and in the second case they decrease. The values of these probabilities control the rate at which the mean connectivity decreases. In the first case, the rate is greater and the self-overlap reaches the value 1 deep inside the ordered phase. In the second case, the rate is very small and the net stabilizes in the disordered phase with self-overlap lower than 1. There is a range for the values of the Φ_k functions that gives the correct rate. The chosen rule produces values in that range. From the theoretical point of view it seems easy to obtain similar results using a fixed connectivity and changing the bias, or modifying both of them simultaneously.

Much future work is open. We think that the order-control coupling parameter proposed in [11] also works for RBN. And vice versa: the proposed method in this article works in this type of binary neural nets. In order to consider biological implications the automata (to be considered as genes) dynamics and the disconnection rule (to be thought of as mutations) should have different characteristic times. We should also include a rule that allows for a possible connection growth, and not simply consider connection loss as we have

done in this article. We think that the point of view considered here can have further applications along these lines. In any case, we can extrapolate our results to a different type of nets that show a clear transition between the ordered and disordered phases with well-defined order and control parameters.

ACKNOWLEDGMENTS

The authors would like to thank C. Molina-París, U. Bastolla, and S. C. Manrubia for their critical reading of the manuscript. This work has been supported by Centro de Astrobiología (CAB).

[1] S. A. Kauffman, *The Origins of Order: Self-Organization and Selection in Evolution* (Oxford University Press, New York 1993).
[2] S.A. Kauffman, J. Theor. Biol. **22**, 437 (1969).
[3] A. Bhattacharjya and S. Liang, Phys. Rev. Lett. **77**, 1644 (1996).
[4] U. Bastolla and G. Parisi, Physica D **115**, 203 (1996); **115**, 219 (1996).
[5] R. Albert and A.-L. Barabási, Phys. Rev. Lett. **84**, 5660 (1998).
[6] S.A. Kauffman, Sci. Am. **265**, 78 (1991).
[7] A.-L. Barabási and R. Albert, Science **286**, 509 (1999).
[8] S.N. Dorogovtsev and J.F.F. Mendes, Phys. Rev. E **62**, 1842 (2000).
[9] S. Bornholdt and K. Sneppen, Phys. Rev. Lett. **81**, 236 (1998).
[10] M. Paczuski, K.E. Bassler, and A. Corral, Phys. Rev. Lett. **84**, 3185 (2000).
[11] S. Bornholdt and T. Rohlf, Phys. Rev. Lett. **84**, 6114 (2000).
[12] K.E. Kürten, J. Phys. A **21**, L615 (1988).
[13] B. Luque and R.V. Solé, Phys. Rev. E **55**, 257 (1997).
[14] S. Maslov and Y.-C. Zhang, Phys. Rev. Lett. **75**, 1550 (1995).
[15] M. Paczuski, S. Maslov, and P. Bak, Phys. Rev. E **53**, 414 (1996).
[16] D. Sornette and I. Dornic, Phys. Rev. E **54**, 3334 (1996).
[17] P. Grassberger and Y.-C. Zhang, Physica A **224**, 169 (1996).
[18] D. Sornette, A. Johansen, and I. Dornic, J. Phys. I **5**, 325 (1995).
[19] B. Derrida, in *Fundamental Problems in Statistical Mechanics VII*, edited by H. van Beijeren (North-Holland, Amsterdam, 1990).
[20] P. Bak, C. Tang, and K. Wiesenfeld, Phys. Rev. Lett. **59**, 381 (1987).
[21] For reviews see P. Bak, *How Nature Works* (Copernicus, New York, 1996); H.J. Jensen, *Self-Organized Criticality* (Cambridge University Press, Cambridge, 1998).
[22] B. Luque and R.V. Solé, Physica A **284**, 33 (2000).